Structural transformation from single-wall to double-wall carbon nanotube bundles

Masatoshi Abe,[1] Hiromichi Kataura,[1] Hiroshi Kira,[1] Takeshi Kodama,[2] Shinzo Suzuki,[2] Yohji Achiba,[2] Ken-ichi Kato,[3]
Masaki Takata,[3,4] Akihiko Fujiwara,[5,6] Kazuyuki Matsuda,[1] and Yutaka Maniwa[1,6,*]

[1]*Department of Physics, Tokyo Metropolitan University, 1-1 Minami-osawa, Hachioji, Tokyo 192-0397, Japan*

[2]*Department of Chemistry, Tokyo Metropolitan University, 1-1 Minami-osawa, Hachioji, Tokyo 192-0397, Japan*

[3]*SPring-8, 1-1-1 Kouto, Mikazuki-cho, Sayo-gun, Hyogo 679-5198, Japan*

[4]*Department of Applied Physics, Nagoya University, Nagoya 464-8603, Japan*

[5]*JAIST, Tatsunokuchi, Ishikawa 923-1292, Japan*

[6]*CREST, JST (Japan Science and Technology Corporation), Japan*

(Received 8 April 2003; published 29 July 2003)

We report an x-ray diffraction (XRD) analysis of the structural transformation from single-wall carbon nanotubes (SWNTs) to double-wall carbon nanotubes (DWNTs) via C_{60}-encapsulating SWNTs (C_{60} peapods). It was shown that the bundle structure of the starting SWNTs retains on this process. The thermal expansion coefficients of DWNTs hardly changed from the pristine SWNTs. The intertube spacing between inner and outer tubes of DWNTs was obtained as 0.36 ± 0.01 nm. This spacing was shown to be determined by the discreteness of the SWNT diameter under a turbostratic constraint between the inner and outer tubes of DWNT at synthesis temperatures.

Recently, interesting synthesis routes to double-wall carbon nanotubes (DWNTs) were reported, in which single-wall carbon nanotubes (SWNTs) encapsulating C_{60} molecules (the so-called peapods) are converted into DWNTs by heating[1] or electron irradiation.[2] The obtained DWNTs would be the same bundle structures as the starting SWNT materials. Therefore, in the light of recent developments in the synthesis and purification technique of SWNTs,[3–6] the method may be most useful for preparing well-defined DWNT bundles at present, as compared with direct synthesis methods.[7,8] However, the structure of DWNT bundles prepared by Bandow's method[1] has not yet been clarified in full detail. Here, we present a structural study of the conversion process from pristine SWNTs to DWNTs through C_{60} peapods by means of x-ray diffraction (XRD). Based on the present XRD studies, the synthesis mechanism of multishell type carbon nanotubes (MWNTs) is discussed.

The starting raw SWNTs were generated by the pulsed laser vaporization of a carbon rod with Ni and Co catalysts in a furnace operated at 1473 or 1523 K.[6] The peapods, which were prepared by a reaction of the purified uncapped SWNTs with C_{60} vapor,[9,10] were converted into DWNTs by heating for 10 h at 1523 K in vacuum, following Bandow's procedure.[1] Transmission electron microscopy confirmed a high yield of the parallel-aligned carbon nanotube packed into bundles with a triangular lattice. All the samples for the XRD measurements were prepared from the same batch of purified SWNT materials. The XRD data were collected using synchrotron radiation with a wavelength of 0.100 nm at beam line BL02B2 of SPring-8 in Japan. Samples were sealed in a quartz glass tube after being evacuated at ~ 800 K to remove adsorbed gases.[11,12] There is no preferential orientation of SWNT axes inside the glass XRD tubes.

Figure 1 shows the typical powder XRD patterns of pristine SWNTs, C_{60} peapods, and DWNTs. The observed peaks can be indexed on the basis of a two-dimensional (2D) triangular lattice[3] consisting of 1D SWNTs. In the figure, we

find marked changes in the XRD profiles on C_{60} encapsulation: the *10* peak around $Q \sim 4.5$ nm^{-1} is strongly depressed, and its onset shifts to the high-Q region. This is evidence of molecular encapsulation inside SWNTs.[11,12] In addition, a new peak appeared upon C_{60} encapsulation around $Q = 6$ nm^{-1}, shown by an arrow, is due to a 1D array of C_{60} molecules inside SWNTs. That is, this peak is due to the so-called 1D C_{60} crystal formed inside each SWNT. The absence of the corresponding peak in the DWNTs implies that the C_{60} peapods are almost fully converted into DWNTs.

To obtain further structural information, we performed detailed simulations of the powder XRD patterns using a ho-
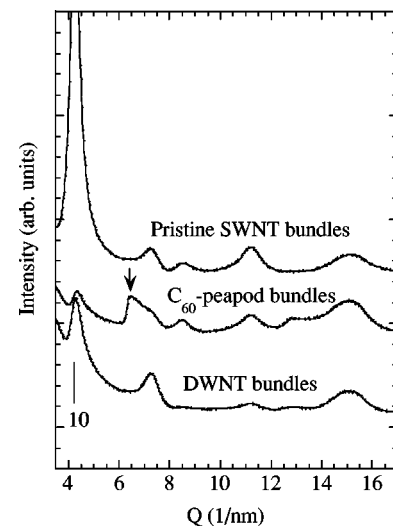

FIG. 1. XRD profiles of (a) pristine empty SWNT bundles, (b) C_{60}-peapod bundles, and (c) DWNT bundles taken at room temperature. These samples were prepared from the same batch of purified SWNTs. An arrow shows the peak due to 1D C_{60} crystals formed inside SWNTs. Q is given by $(4 \pi \sin \theta)/\lambda$, where λ is the x-ray wavelength and 2θ the scattering angle.

mogeneously charged shell model, in which the SWNTs and fullerene molecules are assumed to be thin sheets of homogeneous electron density within the carbon covalent networks. Within the framework of this model, useful structural parameters such as the triangular lattice constant L and tube diameters $2R$ can be deduced. In the present paper, it will be also clarified that the distribution of the "tube diameter averaged within the bundle" is obtained from the simulation, which was neglected in our previous simulations.[11,12]

The diffracted intensity $I_i(Q)$ due to the ith bundle is multiplied by the tube form factor $F_i(Q)$, the Bragg peak profile function $P_G(Q)$, the Lorentz factor $L(Q)$, and the number of equivalent reflections N_G,

$$I_i(Q) \propto \left| \int \rho_i(\vec{r}) \exp(i\vec{Q} \cdot \vec{r}) dV \right|^2 \propto L \cdot |F_i|^2 \sum_{G(i)} (P_{G(i)} N_{G(i)}),$$

(1)

where ρ_i is the electron density and $G(i)$ is the amplitude of reciprocal lattice vector of the ith bundle with the closest packed 2D-triangular lattice. For an empty SWNT, form factor $F_i(Q)$ is given by the zeroth-cylindrical Bessel function $J_0(R_i Q)$. The intertube gap g_i, tube diameter $2R_i$, and bundle thickness t_i were used as the fitting parameters. The triangular lattice constant of the ith bundle is given by $a_i = g_i + 2R_i$. For a case in which there is a distribution of these parameters within a bundle, they must be "averaged" within the bundle. In the following, however, we just set those parameters to representative values for each bundle because this distribution could not substantially affect the simulated profile. The peak function $P_G(Q)$ was assumed by a sum of Gaussian and Lorentzian functions, centered at G, with the same full width at half maximum (FWHM) given by $\Delta Q = 2\pi/t_i$. Here, we further assumed that all the bundles have the same thickness $t_i = t$ for simplicity. Thus, the observed intensity is given by

$$I(Q) = \sum_i I_i(Q) \propto L \sum_i \left[|F_i|^2 \sum_{G(i)} (P_{G(i)} N_{G(i)}) \right].$$

(2)

For empty SWNTs, the simulations were performed for two extreme cases: (a) the gap g_i was fixed, but a distribution of R_i was involved; and (b) the tube radius R_i was fixed but a distribution of g_i was involved. The XRD pattern giving the best agreement with the observed pattern is shown in Fig. 2 for each model. From a comparison of the simulated profiles with experimental XRD patterns, it is clear that model (a) is more favorable. In particular, the profile around $Q = 8$ nm^{-1}, which corresponds to the second node of $J_0(R_i Q)$, is substantially improved. Model (b) failed in the reproduction of the observed sharp dip around $Q = 8$ nm^{-1}. Because the Q value for $J_0(R_i Q) = 0$ is inversely proportional to R_i, as already stressed in a previous paper,[12] it should be noted that the shape and position of the dip give us information about the average tube radius R_i and its distribution in the sample.

The most favorable parameters thus obtained are the following: the average tube radius $\langle R_i \rangle = 0.69 \pm 0.01$ nm, its distribution 0.06 nm defined as the FWHM assuming a
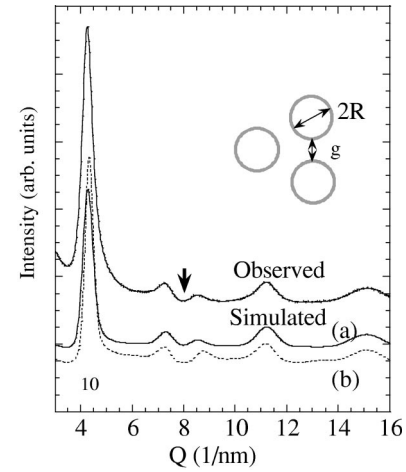

FIG. 2. Observed and simulated XRD profiles of the pristine SWNTs at room temperature. (a) Distribution of SWNT diameter averaged in the bundle was included. (b) The distribution of the intertube gap averaged in the bundle was included.

Gaussian distribution, the bundle thickness 18 nm, and the intertube gap $g = 0.32 \pm 0.01$ nm. This intertube gap g for model (a) is slightly larger than 0.30 ± 0.01 nm for model (b), while the average tube radius hardly depends on the above two models.

A recent UPS (ultraviolet photoemission spectroscopy) experiment succeeded in observations of electronic density of states in essentially the same SWNTs as the present samples, from which a distribution of tube radius R was estimated to have a FWHM of 0.10 nm assuming a Gaussian distribution.[13] This value is almost two times larger than the present estimate. The difference should be ascribed to an inhomogeneity within the bundles, which was not included in the present analysis, because the UPS density of states reflects all the tubes in the sample. Therefore, the distribution of the tube radius within the bundles is roughly estimated as $\sqrt{0.1^2 - 0.06^2} = 0.08$ nm in the present typical sample.

In the case of C_{60} peapods, $F_i(Q)$ is a sum of those for the SWNT and C_{60} molecules inside the SWNT. The sawtooth shape of the peak due to the 1D arrays of C_{60} molecules, i.e., the 1D C_{60} crystals inside SWNTs, which is shown by an arrow around $Q = 6.5$ nm^{-1} in Fig. 1, is evidence of the lack of correlation among the 1D C_{60} crystals in different SWNTs. This is a characteristic in one-dimensional crystals, and an analogous 2D case has been well discussed in turbostratic graphite lacking an interlayer stacking correlation.[14] In such a case, the diffraction have two different origins; diffraction for the 2D-triangular lattice of SWNTs encapsulating C_{60} molecules where the charge density of C_{60} molecules inside SWNTs is smeared along the tube axis; and diffraction for a 1D array of C_{60} molecules inside SWNTs. The simulated pattern is shown in Fig. 3(a), where the same values for the lattice constant and tube diameter as those in the pristine SWNTs were used. The good agreement with the observed pattern implies that the tube diameter and lattice constant are almost unchanged in the C_{60} encapsulation. The best fit was obtained for the inter-C_{60} distance of 0.975 nm and the coherence length of 38 nm for
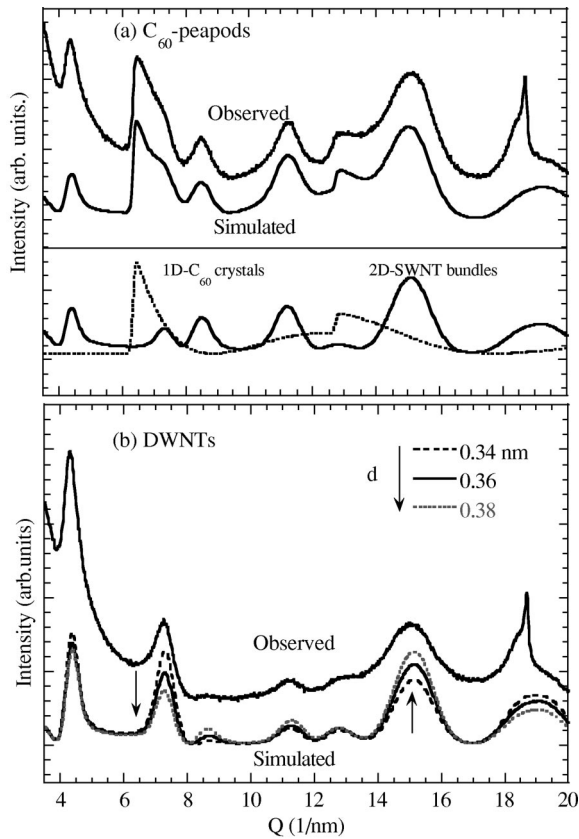
FIG. 3. Observed and simulated XRD profiles of C_{60}-peapod bundles (a) and DWNT bundles (b). The intertube spacing d was changed in simulation of (b).
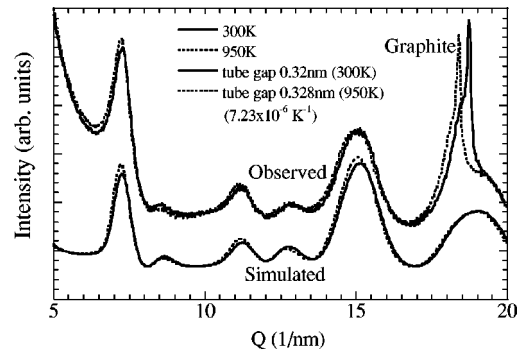

FIG. 4. Observed and simulated XRD profiles of DWNT bundles at 300 K (solid lines) and 950 K (dotted lines). In the simulated profiles, the thermal expansion coefficient of the lattice constant was assumed to be 7.2×10^{-6} K^{-1} and that of the SWNT diameter was neglected. The large peaks around $Q = 18.5$ (1/nm) in the observed profiles are due to impurity graphite.

the 1D C_{60} crystals. A C_{60} filling of about 80% was also obtained, assuming that C_{60} empty sites (defects) are randomly distributed in each SWNT. An alternative model in which the empty SWNT bundles coexist with the fully occupied SWNT bundles was also examined, but the fitting to the observed profiles was not better than the present model.

Now we discuss the DWNTs. The simulations were performed using parameters of the intertube spacing and the filling factor of inner tube. Here, the outer tube diameter, its distribution and the lattice constant were fixed to those values of the pristine SWNT bundles. Examples for the simulated profiles are shown in Fig. 3(b) for the three intertube distances, 0.34, 0.36, and 0.38 nm. The experimental profiles are most successfully reproduced when the intertube distance is 0.36 ± 0.01 nm and the filling factor of the inner tubes 60–65 %. The good agreement of the experimental profile with the simulated one implies that the lattice constant and the outer tube diameter hardly change on the conversion process from the pristine SWNT bundles through C_{60} peapods.

The estimated filling factor of 60–65 % in the present ''DWNT materials'' simply implies that there are empty domains of 35–40 % inside SWNTs. This is due to the fact that the carbon density of the inner tube in ideal DWNTs is higher than that in the C_{60} peapods. The 1D arrays of C_{60} molecules must shrink into DWNTs upon heating. In the case of the present DWNTs with an outer diameter of 1.38 nm and an intertube spacing of 0.36 nm, the reduction factor of the

filling should be 1/0.74, which explains the above estimated value using 80% for the peapods. Therefore, we conclude that the C_{60} molecules fully coalesce into DWNTs inside SWNTs.

Finally, we discuss the thermal expansion of DWNT bundles. The XRD profiles were taken in a temperature range between 300 and 950 K. Examples of the T dependence of XRD profiles are shown in Fig. 4, where small but significant changes can be found. From the negligibly small T dependence of the dip around $Q = 8$ nm^{-1}, it is known that the thermal expansion coefficient of the tube diameter is very small, as in the case of SWNT bundles.[12] Alternatively, the observed change in the profile was solely explained by the thermal expansion coefficient of the triangular lattice constant: $(0.72 \pm 0.25) \times 10^{-5}$ K^{-1}.

The intertube spacing obtained in the present DWNTs is in good agreement with the previous estimate by Raman measurements[1] in the same type of DWNTs. This agreement may suggest a rather weak intertube interaction in DWNTs because Raman spectra in DWNTs are possibly affected by intertube interactions. TEM analysis also showed an intertube spacing of 0.36 nm in MWNTs prepared by a direct arc discharge method.[15] However, values of theoretical calculations[16,17] are quite different. For example, Saito reported that the most stable intertube distance is around 0.342 nm, irrespective of the chirality pair for the inner and outer tubes of DWNTs.[16] The difference must include useful information on the conversion or synthesis process of DWNTs.

The simplest model for the conversion process is as follows. (1) C_{60} molecules coalesce into sp^2-carbon networks at around 1500 K. Because three coordinate-carbon networks would be energetically favorable for the larger curvature, the largest diameter tubes tend to be formed inside the SWNTs. (2) However, these carbon networks must be spaced from the outer SWNTs at least by an interlayer distance, most likely that of turbostratic graphite.[14,18] At the synthesis temperature, this spacing is estimated as 0.355 nm using the thermal expansion coefficient of 2.7×10^{-5} K^{-1} and an intergraphite distance of 0.344 nm at 300 K. (3) Because the SWNT diameter cannot change continuously and is determined by the

tube index (n,m) with integers n and m, the diameter of the inner tube cannot be exactly adapted to the turbostratic interlayer spacing in general.[18] Thus, within the turbostratic constraint, the largest possible tubes should be formed.

We calculated the intertube spacing for 27 pairs of SWNTs in DWNTs with outer diameters of around 1.38 nm under the above turbostratic constraint. The average intertube spacing was 0.361 nm and its standard deviation was 0.004 nm, in good agreement with the observed one. Therefore, the intertube spacing gives us information on the synthesis temperature. In this point of view, many MWNTs may be very defective, because they have intertube spacings comparable to the turbostratic value 0.344 nm at room temperature in spite of the high temperature synthesis, consistent with recent XRD studies on MWNTs.[19–21]

In conclusion, we studied detailed structural conversion process of SWNTs to DWNTs through C_{60} peapods. It was found that the basic bundle structures are retained in this process. It was strongly suggested that the intertube spacing of the resultant DWNTs of 0.36 ± 0.01 nm is primarily determined by the synthesis temperatures, and the inner and outer tubes are loosely coupled to each other.

*Email address: maniwa@phys.metro-u.ac.jp

[1] S. Bandow, M. Takizawa, H. Hirahara, M. Yudasaka, and S. Iijima, Chem. Phys. Lett. **337**, 48 (2001).

[2] J. Sloan, R.E. Dunin-Borkowski, J.L. Hutchison, K.S. Coleman, V.C. Williams, J.B. Claridge, A.P.E. York, C. Xu, S.R. Bailey, G. Brown, S. Friedrichs, and M.L.H. Green, Chem. Phys. Lett. **316**, 191 (2000).

[3] A. Thess, R. Lee, P. Nikolaev, H. Dai, P. Petit, J. Robert, C. Xu, Y.H. Lee, S.G. Kim, A.G. Rinzler, D.T. Colbert, G.E. Scuseria, D. Tomanek, J.E. Fischer, and R.E. Smally, Science **273**, 483 (1996).

[4] C. Journet, W.K. Maser, P. Bernier, A. Loiseau, M. Lamy de la Chapelle, S. Lefrsant, P. Deniard, R. Lee, and J.E. Fischer, Nature (London) **388**, 756 (1997).

[5] K. Tohji, H. Takahashi, Y. Shinoda, N. Shimizu, B. Jeyadevan, I. Matsuoka, Y. Saito, A. Kasuya, S. Ito, and Y. Nishina, J. Phys. Chem. B **101**, 1974 (1997).

[6] H. Kataura, Y. Kumazawa, Y. Ohtsuka, S. Suzuki, Y. Maniwa, and Y. Achiba, Synth. Met. **103**, 2555 (1999).

[7] T. Sugai, H. Omote, S. Banbow, N. Tanaka, and H. Shinohara, J. Chem. Phys. **112**, 6000 (2000).

[8] R. Bacsa, C. Laurent, A. Peigney, W.S. Bacsa, T. Vaugien, and A. Roussert, Chem. Phys. Lett. **323**, 566 (2001).

[9] H. Kataura, Y. Maniwa, T. Kodama, K. Kikuchi, H. Hirahara, K. Suenaga, S. Iijima, S. Suzuki, Y. Achiba, and W. Kraetschmer, Synth. Met. **121**, 1195 (2001).

[10] H. Kataura, Y. Maniwa, M. Abe, A. Fujiwara, T. Kodama, K. Kikuchi, H. Imahori, Y. Misaki, S. Suzuki, and Y. Achiba, Appl. Phys. A: Mater. Sci. Process. **74**, 349 (2002).

[11] Y. Maniwa, Y. Kumazawa, Y. Saito, H. Tou, H. Kataura, H. Ishii, S. Suzuki, Y. Achiba, A. Fujiwara, and H. Suematsu, Jpn. J. Appl. Phys. **38**, L668 (1999).

[12] Y. Maniwa, R. Fujiwara, H. Kira, H. Tou, H. Kataura, S. Suzuki, Y. Achiba, E. Nishibori, M. Takata, M. Sakata, A. Fujiwara, and H. Suematsu, Phys. Rev. B **64**, 241402(R) (2001).

[13] H. Ishii *et al.* (private communication).

[14] B.E. Warren, Phys. Rev. **59**, 693 (1941).

[15] X. Sun, C.H. Kiang, M. Endo, K. Takeuchi, T. Furuta, and M.S. Dresselhaus, Phys. Rev. B **54**, R12 629 (1996).

[16] R. Saito, R. Matsuo, T. Kimura, G. Dresselhaus, and M.S. Dresselhaus, Chem. Phys. Lett. **348**, 187 (2001).

[17] J.C. Charlier and J.P. Michenaud, Phys. Rev. Lett. **70**, 1858 (1993).

[18] *Science of Fullerenes and Carbon Nanotubes*, edited by M.S. Dresselhaus, G. Dresselhaus, and P.C. Eklund (Academic Press, New York, 1995), p. 756.

[19] O. Zhou, R.M. Fleming, D.W. Murphy, C.H. Chen, R.C. Haddon, A.P. Ramurez, and S.H. Glarum, Science **263**, 1744 (1994).

[20] S. Bandow, Jpn. J. Appl. Phys. **36**, L1403 (1997).

[21] Y. Maniwa, R. Fujiwara, H. Kira, H. Tou, E. Nishibori, M. Takata, M. Sakata, A. Fujiwara, X. Zhao, S. Iijima, and Y. Ando, Phys. Rev. B **64**, 073105 (2001).